

Vaccines

How to cite: *Angew. Chem. Int. Ed.* **2021**, 60, 9467–9473

International Edition: doi.org/10.1002/anie.202015362

German Edition: doi.org/10.1002/ange.202015362

Sterilizing Immunity against SARS-CoV-2 Infection in Mice by a Single-Shot and Lipid Amphiphile Imidazoquinoline TLR7/8 Agonist-Adjuvanted Recombinant Spike Protein Vaccine**

Sonia Jangra⁺, Jana De Vrieze⁺, Angela Choi⁺, Raveen Rathnasinghe, Gabriel Laghlali, Annemiek Uvyn, Simon Van Herck, Lutz Nuhn, Kim Deswarte, Zifu Zhong, Niek N. Sanders, Stefan Lienenklaus, Sunil A. David, Shirin Strohmeier, Fatima Amanat, Florian Krammer, Hamida Hammad, Bart N. Lambrecht, Lynda Coughlan, Adolfo García-Sastre, Bruno G. De Geest,* and Michael Schotsaert*

Abstract: The search for vaccines that protect from severe morbidity and mortality because of infection with severe acute respiratory syndrome coronavirus 2 (SARS-CoV-2), the virus that causes coronavirus disease 2019 (COVID-19) is a race against the clock and the virus. Here we describe an amphiphilic imidazoquinoline (IMDQ-PEG-CHOL) TLR7/8 adjuvant, consisting of an imidazoquinoline conjugated to the chain end of a cholesterol-poly(ethylene glycol) macromolecular amphiphile. It is water-soluble and exhibits massive translocation to lymph nodes upon local administration through binding to albumin, affording localized innate immune activation and reduction in systemic inflammation. The adjuvant activity of IMDQ-PEG-CHOL was validated in a licensed vaccine setting (quadrivalent influenza vaccine) and an experimental trimeric recombinant SARS-CoV-2 spike protein vaccine, showing robust IgG2a and IgG1 antibody titers in mice that could neutralize viral infection *in vitro* and *in vivo* in a mouse model.

Introduction

Severe acute respiratory syndrome coronavirus 2 (SARS-CoV-2), as the causative agent of coronavirus disease 2019, also known as COVID-19, is a beta-coronavirus which belongs to the family of *Coronaviridae* and is currently responsible for the third human coronavirus outbreak in the past 20 years.^[1–3] Therapeutic drugs are of limited use in the clinic and effective mass immunization campaigns that induce long lasting immunity are generally considered crucial to mitigate the ongoing pandemic. More than hundred candidate vaccines, consisting of multiple vaccine types such as recombinant viral epitopes, adenovirus-based vectors, purified inactivated or live-attenuated virus, virus like particles and DNA or RNA based vaccine formulations, are currently being investigated.^[4,5] At present mRNA-based vaccines formulated in lipid nanoparticles, recombinant protein-based and inactivated virus-based vaccines as well as viral vector-

[*] Dr. S. Jangra,^[+] A. Choi,^[+] R. Rathnasinghe, G. Laghlali, S. Strohmeier, F. Amanat, Prof. Dr. F. Krammer, Prof. Dr. L. Coughlan, Prof. Dr. A. García-Sastre, Prof. Dr. M. Schotsaert
Department of Microbiology
Icahn School of Medicine at Mount Sinai
New York, NY (USA)
E-mail: michael.schotsaert@mssm.edu

J. De Vrieze,^[+] A. Uvyn, Dr. S. Van Herck, Dr. Z. Zhong, Prof. Dr. B. G. De Geest
Department of Pharmaceutics, Ghent University
Ghent (Belgium)
E-mail: br.degeest@ugent.be

A. Choi,^[+] R. Rathnasinghe, S. Strohmeier, F. Amanat
Graduate School of Biomedical Sciences
Icahn School of Medicine at Mount Sinai, New York, NY (USA)

K. Deswarte, Prof. Dr. H. Hammad, Prof. Dr. B. N. Lambrecht
Department of Internal Medicine and Pediatrics, Ghent University and VIB Center for Inflammation Research
Zwijnaarde (Belgium)

Prof. Dr. N. N. Sanders
Laboratory for Gene Therapy, Ghent University
Merelbeke (Belgium)

Dr. S. Lienenklaus
Institute for Laboratory Animal Science, Institute of Immunology
Hannover Medical School, Hannover (Germany)

Dr. S. A. David
Virovax, Lawrence, KS (USA)

Prof. Dr. B. N. Lambrecht
Department of Pulmonary Medicine, Erasmus Medical Center
Rotterdam (The Netherlands)

Prof. Dr. A. García-Sastre, Prof. Dr. M. Schotsaert
Global Health and Emerging Pathogen Institute
Icahn School of Medicine at Mount Sinai, New York, NY (USA)

Prof. Dr. A. García-Sastre
Department of Medicine, Division of Infectious Diseases
Icahn School of Medicine at Mount Sinai, New York, NY (USA)
and
The Tisch Cancer Institute
Icahn School of Medicine at Mount Sinai, New York, NY (USA)

Dr. L. Nuhn
Max Planck Institute for Polymer Research, Ackermannweg 10,
55128 Mainz (Germany)

[+] These authors contributed equally to this work.

[**] A previous version of this manuscript has been deposited on a preprint server (<https://www.biorxiv.org/content/10.1101/2020.10.23.344085v1>).

 Supporting information and the ORCID identification number(s) for the author(s) of this article can be found under:
<https://doi.org/10.1002/anie.202015362>.

based vaccines have reached late stage of clinical development and are entering the market. For these vaccines, pre-clinical data in animal models and phase 3 clinical trials^[6,7] also support the hypothesis that these vaccines can effectively prevent severe illness upon viral infection. However, little is known about whether recombinant protein vaccines are capable of conferring protective immunity. In contrast to the aforementioned mRNA and viral vector-based vaccines, recombinant protein vaccines are simpler as they consist of a single entity antigen and do not require antigen expression in the vaccinees. mRNA vaccines show promising results. However, the need for formulation into lipid nanoparticles, required to overcome the barrier of the endosomal membrane before the mRNA reaches its molecular target the cytoplasm, poses considerable challenges in the context of manufacturing and storage.^[8] Hence, exploring the viability of a recombinant protein COVID-19 vaccine might be of considerable relevance.

SARS-CoV-2 encodes four major structural proteins, spike (S), membrane (M), nucleocapsid (N), and envelope (E). The spike protein comprises a homotrimeric structure which is present on the surface of the virus and facilitates the viral attachment and entry into the host via human angiotensin-converting enzyme 2 (hACE-2) receptors via its receptor-binding domain (RBD).^[9–11]

Owing to its involvement in viral entry, the S protein is a major target for current vaccine development against SARS-CoV-2.^[5] Therefore, in this study we explored the recombinant SARS-CoV-2 S protein as a potential vaccine candidate. As recombinant protein antigens are poorly immunogenic and are incapable of mounting antigen-specific immunity of sufficient quality, amplitude and duration, co-administration of adjuvants that shape B cell and T cell responses are indispensable. Adjuvants like alum and oil-in-water emulsions can act through a multitude of mechanisms. More defined small molecule adjuvants that potently activate innate immune cells by triggering specific innate immune receptors might be more relevant for anti-viral vaccine design. The Toll-like receptors 7 and 8 (TLR7/8) are widely distributed amongst innate immune cell subsets over a broad range of species.^[12] Akin to be an endosomal pattern recognition receptor for viral RNA, triggering of these receptors provokes robust type I interferon production that can skew a Th1-type adaptive immune response against co-administered antigen.^[13] The latter are characterized by robust antibody titers capable of inducing viral neutralization through a variety of mechanisms, including Fc-mediated innate immune killing as well as inducing CD4+ and CD8+ T-cell based immunological memory. Moreover, vaccines adjuvanted with TLR7/8 ligands have been shown to confer enhanced protective immunity in both mouse and non-human primate models.^[14,15]

Being well-defined small molecules, imidazoquinolines are a class of TLR7/8 agonists^[16] that hold a massive technological advantage in terms of production and physicochemical stability. However, their pharmacokinetic profile is characterized by rapid systemic dissemination upon local (subcutaneous or intramuscular) administration, thereby causing unwanted innate immune activation at multiple distal

tissues,^[17] which is currently a strong limitation for applying imidazoquinoline TLR7/8 agonists in mass immunization campaigns. We and others have reported on strategies to alter the bio-distribution of imidazoquinolines through chemical conjugation to a synthetic carrier that limits systemic circulation but confers robust translocation to immune-inducing sites in sentinel lymph nodes.^[17–23]

In the present work, we report on a novel amphiphilic carrier for imidazoquinoline (IMDQ) TLR7/8 agonists with high translational potential, based on conjugation of a single imidazoquinoline to the chain end of a cholesteryl-polyethylene glycol macromolecular amphiphile (IMDQ-PEG-CHOL; Figure 1 A). This design mediates binding to serum proteins such as albumin^[17,21–23] (Figure 1 B) and in contrast to pure lipidation, the conjugate is well water-soluble.

We demonstrate that IMDQ-PEG-CHOL is a potent adjuvant which enhances vaccine efficiency and induces robust Th1 skewed antibody responses in mice when delivered as a single shot with either admixed S protein (for SARS-CoV-2) or seasonal quadrivalent inactivated influenza virus vaccine (QIV, for influenza). Moreover, IMDQ-PEG-CHOL was able to confer protection in SARS-CoV-2 or influenza virus (H1N1)-infected mice. In this context, it is noteworthy that in contrast to human ACE-2, murine ACE-2 is not targeted by wild type SARS-CoV-2 virus because of species-specific variations in ACE-2 receptors between mouse and human. Here we made use of a mouse model where hACE-2 was introduced through an adenoviral vector, which allows for subsequent replication of SARS-CoV-2 upon infection in the airways of transduced mice.^[24]

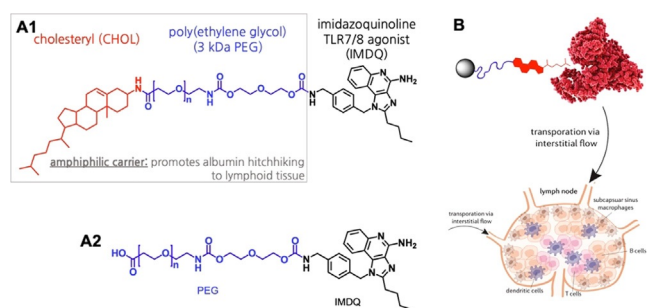


Figure 1. A) Molecular structure of (A1) IMDQ-PEG-CHOL and (A2) IMDQ-PEG. Conjugation was performed by amide bond formation between, respectively cholesterylamine and PEG and PEG and IMDQ. B) Representation of albumin hitchhiking-mediated lymphatic transportation.

Results and Discussion

The imidazoquinoline 1-(4-(aminomethyl)benzyl)-2-butyl-1*H*-imidazo[4,5-*c*]quinolin-4-amine (IMDQ)^[25] was conjugated to cholesteryl-poly(ethylene glycol) (PEG-CHOL), yielding IMDQ-PEG-CHOL. As a control, non-amphiphilic IMDQ-PEG was synthesized. (Figure 1 A) PEG with a molecular weight of 3 kDa was chosen as an optimal compromise between water solubility and drug load. Characterization of the conjugate was performed by matrix assisted laser desorption/ionization–time of flight (MALDI-ToF) (Support-

ing Information, Figure S1) analysis whereas high pressure liquid chromatography (HPLC) analysis (Supporting Information, Figure S2) proved absence of free soluble non-conjugated IMDQ. Both IMDQ-PEG-CHOL and IMDQ-PEG were water-soluble, but only IMDQ-PEG-CHOL showed affinity towards albumin as measured by biolayer interferometry (Figure 2A). On the in vitro level, the presence of the CHOL motif dramatically improved cellular uptake by DC2.4 (Figure 2B,C; note that for imaging purpose, IMDQ was replaced by the fluorescent probe Cyanine5), a murine model mouse dendritic cell line. Furthermore, compared to IMDQ-PEG, IMDQ-PEG was more potent in inducing NF- κ B activation in a reporter cell

line (Figure 2D), while being non-toxic within the tested experimental window (Figure 2E). We attribute this to the ability of the cholesterol motif to interact with the phospholipid cell membrane. Note that the drop in activity of conjugated IMDQ relative to native IMDQ is in accordance to our earlier findings.^[17–19]

On the in vivo level, using a transgenic luciferase-reporter mouse model for IFN β -production,^[26] we found that local administration (subcutaneous injection into the footpad) of IMDQ-PEG-CHOL, in contrast to unformulated IMDQ, dramatically reduced systemic innate immune activation, while focusing its activity to the site of injection and the draining (popliteal) lymph node (Figure 3A). For quantifica-

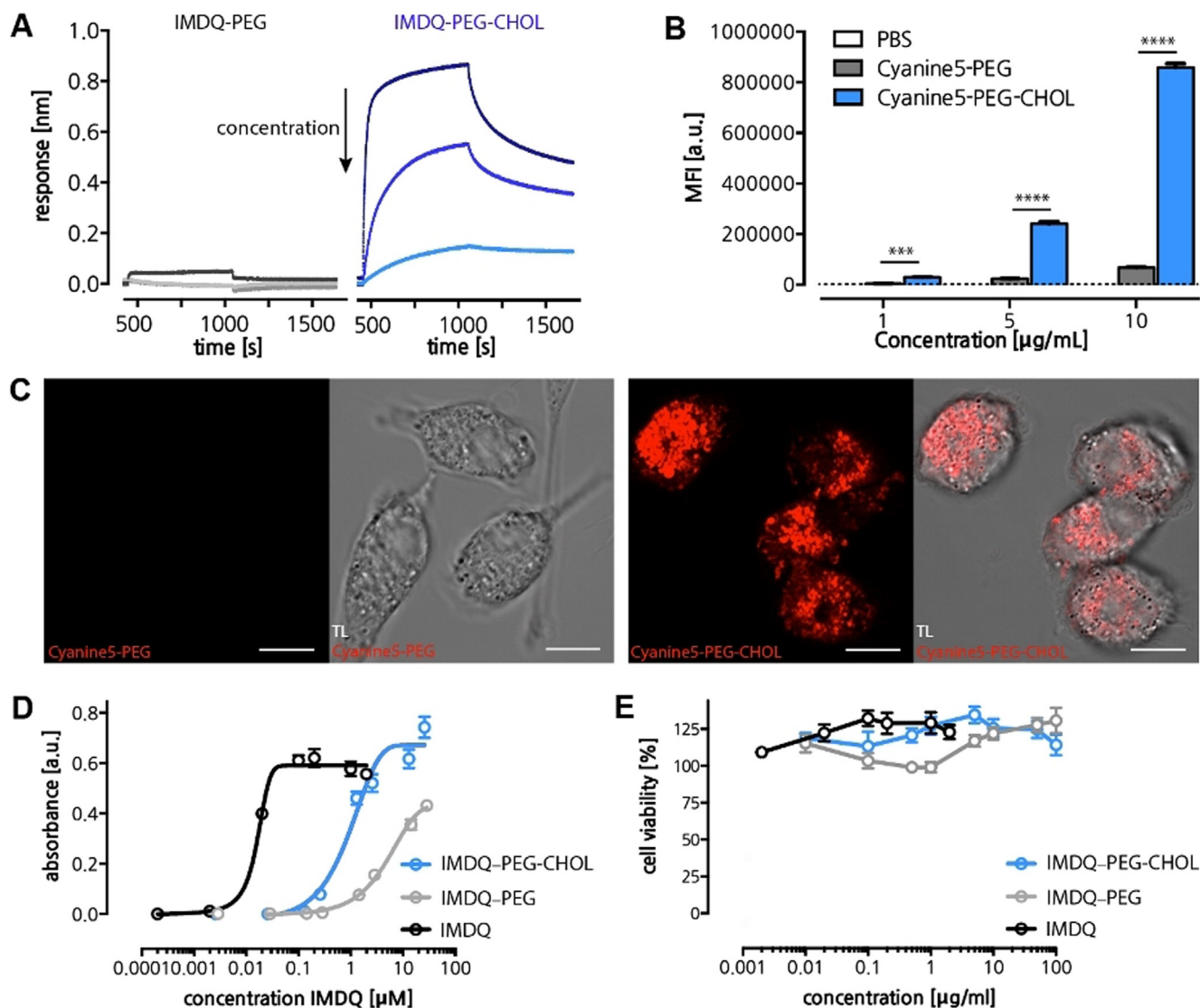


Figure 2. A) Biolayer interferometry (BLI) sensorgrams of non-amphiphilic IMDQ-PEG and amphiphilic IMDQ-PEG-CHOL binding to albumin-coated sensors. A dilution series of 50, 10, and 5 mg mL⁻¹ (dark to light color code, as marked by the black arrow) was measured. Sensors were dipped into a PEG-or lipid-PEG solution at the 500 s time point, which marks the onset of adsorption. At the 1125 s time point, sensors were dipped into PBS, which marks the onset of desorption. B) Flow cytometry analysis of association between DC2.4 cells and Cyanine5-PEG, Cyanine5-PEG-CHOL, respectively. ($n = 3$; Student t-test, ****: $p < 0.0001$, ***: $p < 0.001$) C) Confocal microscopy images of DC2.4 cells incubated for 24 h at 37 °C with Cyanine5-PEG and Cyanine5-PEG-CHOL. Left panel represents the Cyanine5 channel, right panel represents the overlay of the Cyanine5 and transmitted light channels. Scale bar: 15 μ m. D) TLR agonistic activity of IMDQ-PEG-CHOL, IMDQ-PEG and native IMDQ measured as NF- κ B activation using the RAW-Blue reporter cell assay. ($n = 6$, mean + SD). E) Cytotoxicity of IMDQ-PEG-CHOL, IMDQ-PEG and native IMDQ, measured by MTT assay ($n = 6$, mean + SD).

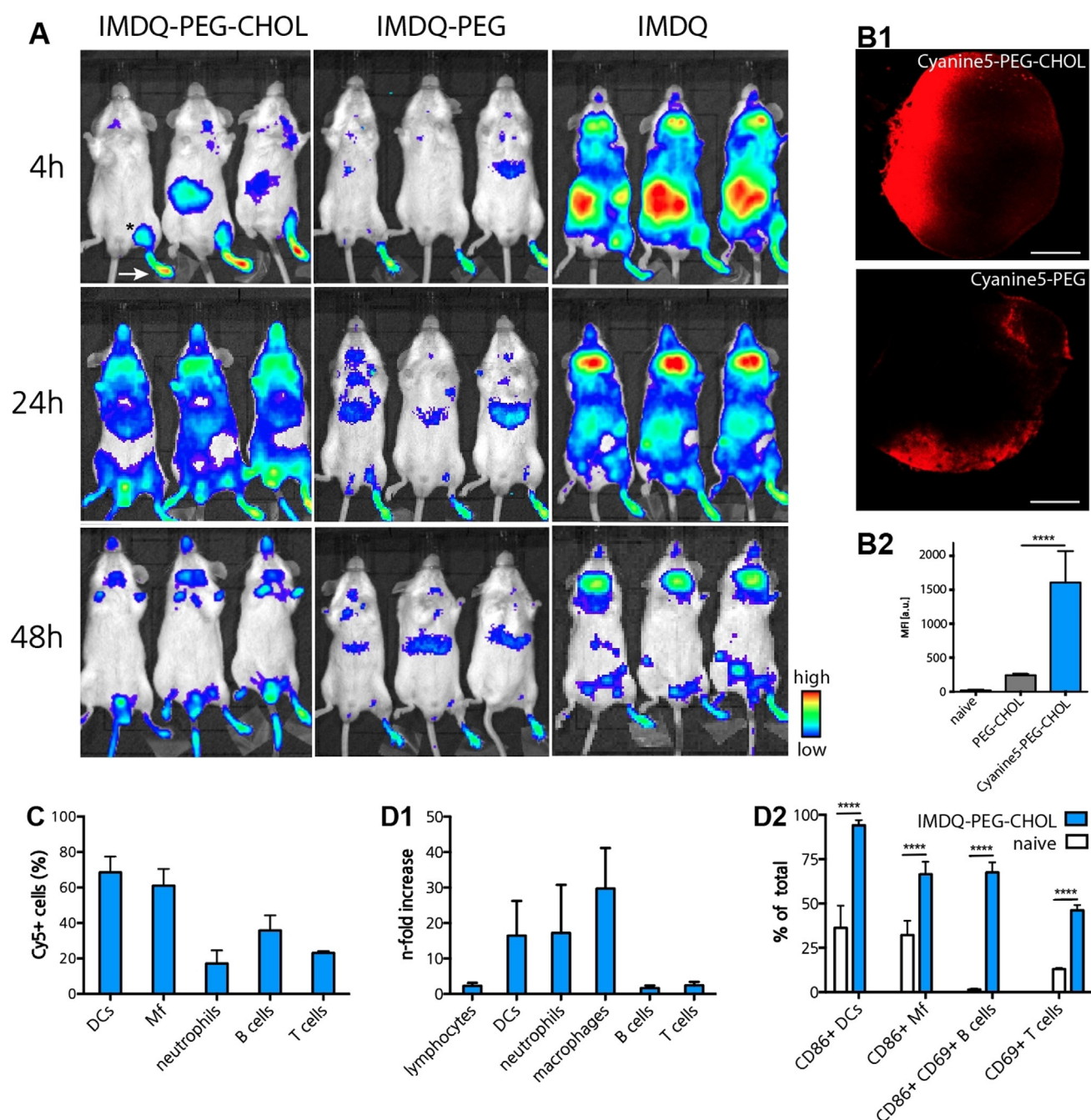


Figure 3. A) Bioluminescence images of luciferase reporter mice ($IFN\beta + /\Delta\beta\text{-luc}$); images taken 4, 24 and 48 h post footpad injection of IMDQ-PEG-CHOL, IMDQ-PEG and native IMDQ. B1) Confocal microscopy images of lymph node tissue sections 48 h post subcutaneous injection of Cyanine5-PEG-CHOL, respectively Cyanine5-PEG, into the footpad of mice. Scale bar: 100 μm . B2) Flow cytometry analysis of the draining popliteal lymph node 48 h post subcutaneous injection of Cyanine5-PEG-CHOL, respectively Cyanine5-PEG into the footpad of mice. ($n = 3$, mean + SD; Student's t-test: ****: $p < 0.0001$) C) Translocation of Cyanine5-PEG-CHOL to the draining popliteal lymph node analyzed 24 h post injection into the footpad, measured by flow cytometry. ($n = 6$, mean + SD) D) Flow cytometry analysis of the innate immune response in the draining popliteal lymph node 24 h post injection of IMDQ-PEG-CHOL into the footpad (D1) Relative increase in innate immune cell subsets, B and T cell numbers relative to a naive control and (D2) maturation/activation of innate immune cell subsets, B and T cells ($n = 6$, mean + SD; Student's t-test: ****: $p < 0.0001$).

tion of the luminescence imaging data, we refer to the Supporting Information, Figure S3. Interestingly, the CHOL motif appeared crucial for mediating lymphatic translocation as the IMDQ-PEG control induced very limited activity in the draining lymph node. To further support this, we performed

microscopic (Figure 3B1) and flow cytometry (Figure 3B2) analysis of popliteal lymph nodes of mice that received fluorescent Cyanine5-PEG-CHOL or Cyanine-PEG, respectively. These experiments revealed a dramatic increase in fluorescence when the conjugates contained the CHOL motif.

A more detailed analysis of immune cells subsets in the draining lymph node revealed that vast percentages of lymphocytes, notably over 50% of dendritic cells (DCs) and macrophages (Mφ), as well as 40% of B cells, were targeted by Cyanine5-PEG-CHOL (Figure 3C). In a similar experimental setting, IMDQ-PEG-CHOL induced recruitment (Figure 3D1) and robust activation (Figure 3D2) of immune cells. Taken together, these data support our hypothesis that IMDQ-PEG-CHOL is a potent adjuvant that focuses its activity to draining lymphoid tissue, combined with a promising safety profile.

We evaluated the potential of IMDQ-PEG-CHOL to adjuvant a licensed vaccine, that is, the quadrivalent influenza vaccine (QIV), in a well-established preclinical vaccination-infection model. Hereto we vaccinated BALB/c mice with each of 1.5 μg of QIV with or without 100 μg of IMDQ-PEG-CHOL or PEG-CHOL as a control. The study protocol is outlined in Figure 4A. Six mice in each group received a total of 100 μL vaccine-adjuvant mixture, intramuscularly, divided over both hind legs and the blood was collected 3 weeks post vaccination, followed by serological assays. No adverse effects as a result of vaccination were observed. For detection of influenza-specific antibodies induced by the QIV vaccines, we used vaccine antigen to coat enzyme-linked immunosorbent

assay (ELISA) plates. The total IgG antibody titers in mice which received QIV only or QIV + PEG-CHOL were very low as compared to the mice vaccinated with QIV + IMDQ-PEG-CHOL (also shown as area under curve (AUC) in the Supporting Information, Figure S4). Unadjuvanted QIV and PEG-CHOL admixed QIV resulted mainly in vaccine-specific IgG1 antibodies, whereas IMDQ-PEG-CHOL resulted in a balanced IgG1/IgG2a response as shown in Figure 4B. Interestingly, QIV + PEG-CHOL resulted in even lower antibody responses than QIV alone, an observation we confirmed in an independent vaccination experiment (data not shown). The sera from four out of six mice that received QIV + IMDQ-PEG-CHOL could efficiently inhibit hemagglutination of chicken red blood cells (RBC) in vitro, by A/Singapore/gp1908/2015 IVR-180, the H1N1 virus component in QIV, with hemagglutination inhibition (HI) titers outperforming those of the other immunized groups (Figure 4C).

Next, the immunized mice were challenged with a hundred-fold half-lethal dose (LD₅₀) of IVR-180 (H1N1) virus to examine the magnitude of protection against viral infection in vivo. The lungs were harvested from three mice in each group 5 days post challenge to determine lung virus titers. Consistent with the ELISA and HI data, mice immunized with

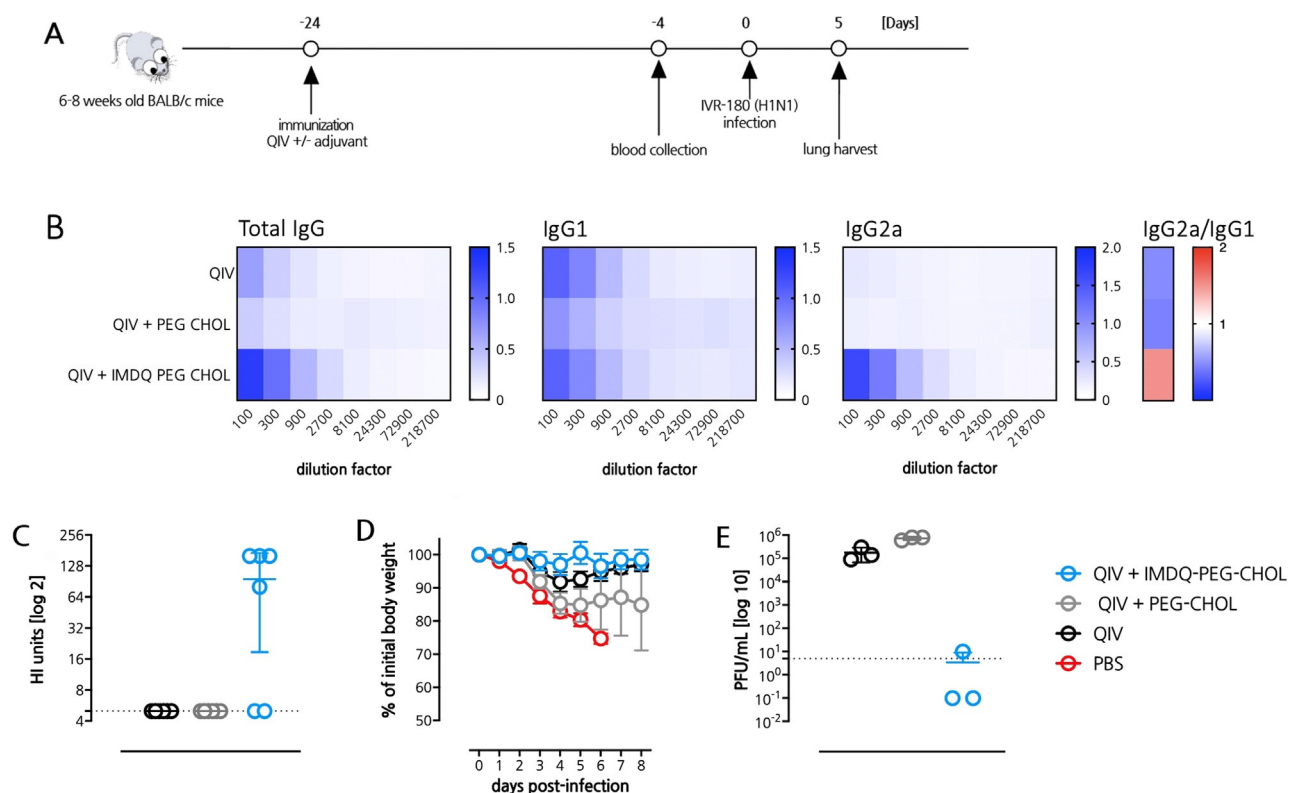


Figure 4. IMDQ-PEG-CHOL induces a balanced neutralizing antibody response to IVR-180 [Influenza A/Singapore/gp1908/2015 (H1N1)] infection. A) Outline of the QIV immunization and influenza virus challenge study. B) Vaccine-specific ELISA titers (titers are expressed on the X axis as the reciprocal of the dilution factor) for total IgG, IgG1 and IgG2a and IgG2a/IgG1 ratio (based on the AUC (OD at 450 nm) curve of the individual serum samples) in mice sera collected 3 weeks post-vaccination. C) Control versus immunized sera analyzed for HI titers by hemagglutination inhibition assay, using 4 haemagglutination units of IVR-180 virus. D) Body weight loss of mice reported as percentage of initial body weight after challenge with 100 LD₅₀ (18 000 PFU) of IVR-180 virus. E) Viral lung titers after challenge with 100LD₅₀ (18 000 PFU) of IVR-180 virus. Data are represented as plaque-forming-unit (PFU) mL⁻¹ (geometric mean + SD). Lungs were harvested on day-5 post infection with IVR-180 virus.

QIV + IMDQ-PEG-CHOL exhibited best reduction in viral lung titers as evidenced by an almost negligible number of plaques when compared to other groups (Figure 4E). This was also reflected in the optimal protection from body weight loss of QIV + IMDQ-PEG-CHOL mice after viral challenge (Figure 4D). In conclusion, our novel adjuvant IMDQ-PEG-CHOL was able to offer excellent control of viral infection and therefore, in combination with the right antigen, might also hold promise to confer protective immunity against other respiratory viruses such as SARS-CoV-2.

We next investigated the potential of IMDQ-PEG-CHOL to adjuvant recombinant SARS-CoV-2 S protein. For this purpose, BALB/c mice were immunized intramuscularly with 6 μ g of recombinant trimeric spike protein either unadjuvanted or adjuvanted with IMDQ-PEG-CHOL or with equivalent amounts of MF59-like water-in-oil vaccine AddaVax as a control established vaccine adjuvant. The recombinant vaccine consisted of the ectodomain of the SARS-CoV-2 spike protein from which the polybasic cleavage site was removed. Stabilizing prolines were added at positions 986 and 987 and trimerization was promoted by fusion to a T4 trimerization domain (see the Supporting Information, Methods section for more details). The study protocol is outlined in Figure 5A. Serum was collected after 21 days post immunization and analyzed for Spike protein specific IgG titers. Whereas non-immunized mice evidently did not show any detectable spike protein-specific titers in their sera, immunization with S protein induced Spike protein-specific titers in all groups (Figure 5B), also shown as area under the curve (AUC) titers in Supplementary Figure 54. The total S protein-specific IgG titers were found to be the highest in the IMDQ-PEG-CHOL adjuvanted group. Additionally, Spike protein + IMDQ-PEG-CHOL immunization resulted in a higher IgG2a/IgG1 ratio, suggesting a more potent Th1 immune response and more efficient class switching towards IgG2a as compared to spike protein only or spike protein + AddaVax immunization.

Next, the sera from vaccinated mice were used to test the ability to inhibit SARS-CoV-2 infection *in vitro*. Although immunization with non-adjuvanted S protein was able to induce some IgG titers, it was found ineffective in neutralizing viral infection of Vero E6 cells *in vitro* in a microneutraliza-

tion assay (Figure 5C1-2). By contrast, serum of mice immunized with spike protein + IMDQ-PEG-CHOL was able to neutralize >50% of SARS-CoV-2 virus infection in this assay, which was also significantly higher than the serum of mice immunized with spike protein + AddaVax. Therefore, as has been reported for human convalescent sera, higher anti-spike ELISA titers correlate with microneutralization titers (reference).^[27]

Finally, we investigated to what extent S protein + IMDQ-PEG-CHOL immunization is able to confer protection against a SARS-CoV-2 viral challenge. As mice do not express the hACE-2 receptor that is needed for the virus to infect the host, we first transduced immunized mice with an adenoviral vector encoding for hACE-2 by intranasal installation. Four days later, mice were challenged with SARS-CoV-2 virus and again 4 days later, lungs were harvested, and the residual viral infection was quantified by a plaque assay. Interestingly, whereas non-adjuvanted Spike protein could not confer any protection, relative to the non-immunized group, Spike protein + IMDQ-PEG-CHOL vaccination conferred sterilizing immunity against the SARS-CoV-2 infection with plaque numbers below the detection limit (Figure 5D), and performed significantly better than spike protein + AddaVax immunization, which correlates with the higher microneutralization titers observed in the spike protein + IMDQ-PEG-CHOL group (Figure 5C1-2).

Conclusion

We have shown in this work that IMDQ-PEG-CHOL is a potent adjuvant with enhanced safety profile that induced innate immune activation in lymphoid tissue upon local administration. Whereas IMDQ in soluble, unformulated form, rapidly enters systemic circulation, conjugation to a lipid-polymer amphiphile prevents the latter while promoting translocation to the draining lymph node, likely through binding to albumin in the interstitial flow. In mouse models, we have demonstrated that a single immunization with QIV or S protein adjuvanted with IMDQ-PEG-CHOL induced robust Th1 skewed antibody responses. Importantly, vaccination with QIV and S protein adjuvanted with IMDQ-PEG-

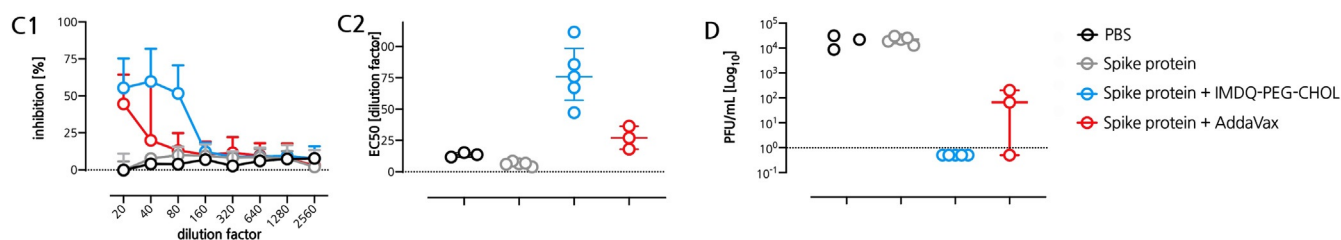


Figure 5. IMDQ-PEG-CHOL induces a balanced neutralizing antibody response to SARS-CoV-2 infection. A) Outline of the Spike protein vaccination and SARS-CoV-2 challenge. B) ELISA titers (titers are expressed on the X axis as the reciprocal of the dilution factor) for total IgG, IgG1, and IgG2a and IgG2a/IgG1 ratio (based on the AUC (OD at 450 nm) curve of the individual serum samples) in mice sera collected 3 weeks post-vaccination. C) Control versus vaccinated sera examined for presence of virus-neutralizing antibodies by microneutralization assay, using 100 tissue culture infectious dose 50 (TCID₅₀) of SARS-CoV-2 virus. The outcome is represented as a percentage inhibition of viral growth in (C1) and as the half maximal inhibitory concentration IC₅₀ calculated by a non-linear regression analysis of percentage inhibition curve in (C2). D) Viral lung titers represented as Plaque-forming-unit (PFU) mL⁻¹ (geometric mean with geometric SD). The Ad5-hACE2 transduced mice were challenged with 5 × 10⁴ PFU of SARS-CoV-2 and the lungs were harvested on day-4 post infection.

CHOL resulted in virus-specific neutralizing antibodies and control of viral infection after challenge with influenza and SARS-CoV-2 viruses, respectively. Whereas we are aware of the limitations of the present studies, we do believe that the overarching message that single vaccination with a properly adjuvanted recombinant S protein-based vaccine is able to induce protective immunity in a mouse model, is of great relevance with regard to broadening the arsenal of emerging COVID-19 vaccines.

Furthermore, the concept of PEG-CHOL conjugation could be applied to other small molecule drugs that have the lymph node as a target tissue, including innate receptor agonists, immune checkpoints blockers and chemotherapeutics.

Acknowledgements

This work was partly funded by CRIP (Center for Research on Influenza Pathogenesis), a NIAID funded Center of Excellence for Influenza Research and Surveillance (CEIRS, contract no. HHSN272201400008C), by SEM-CIVIC, a NIAID funded Collaborative Influenza Vaccine Innovation Center (contract no. 75N93019C00051), by a supplement to NIAID contract 75N93019C00045, by NIAID grants U01AI124297 and P01AI097092, by FASTGRANT 2176, and by the generous support of the JPB Foundation, the Open Philanthropy Project (research grant 2020–215611 (5384)) and anonymous donors to A.G.-S. This work was supported in part by NIAID R21AI157606 (L.C.). Work in the Krammer laboratory was supported by the NIAID Centers of Excellence for Influenza Research and Surveillance (CEIRS) contract HHSN272201400008C (F.K., for reagent generation), Collaborative Influenza Vaccine Innovation Centers (CIVIC) contract 75N93019C00051 (F.K., for reagent generation), and the generous support of the JPB foundation, the Open Philanthropy Project (no. 2020–215611) and other philanthropic donations. B.G.D.G. acknowledges funding from the European Research Council (ERC) under the European Union's Horizon 2020 research and innovation program (grant N 817938). We also thank Randy Albrecht and Carles Martinez for support with the BSL3 facility and procedures at the ISMMS and Richard Cadagan for excellent technical assistance.

Conflict of interest

A.G.-S. is inventor in patents on influenza and COVID-19 vaccines owned by the Icahn School of Medicine at Mount Sinai. The laboratory of A.G.-S. has research agreements on the study of viral vaccines and prophylaxis with Avimex, Pfizer, and 7Hills Pharma. A.G.-S. is a consultant for Avimex and Esperovax.

Keywords: amphiphiles · COVID-19 · innate immunity · SARS-CoV-2 · vaccines

- [1] M. Letko, A. Marzi, V. Munster, *Nat. Microbiol.* **2020**, *5*, 562–569.
- [2] N. Zhu, D. Zhang, W. Wang, X. Li, B. Yang, J. Song, et al., *N. Engl. J. Med.* **2020**, *382*, 727–733.
- [3] F. Wu, S. Zhao, B. Yu, Y.-M. Chen, W. Wang, Z.-G. Song, et al., *Nature* **2020**, *579*, 265–269.
- [4] F. Krammer, *Nature* **2020**, *586*, 516–527.
- [5] T. Ye, Z. Zhong, A. García-Sastre, M. Schotsaert, B. G. De Geest, *Angew. Chem. Int. Ed.* **2020**, *59*, 18885–18897; *Angew. Chem.* **2020**, *132*, 19045–19057.
- [6] F. P. Polack, S. J. Thomas, N. Kitchin, J. Abaslon, A. Gurtman, S. Lockhart, et al., *N. Engl. J. Med.* **2020**, *383*, 2603–2615.
- [7] E. E. Walsh, R. W. Freck, A. R. Falsey, N. Kitchin, J. Absalon, A. Gurtman, *N. Engl. J. Med.* **2020**, *383*, 2439–2450.
- [8] D. J. A. Crommelin, T. J. Anchordoquy, D. B. Volkin, W. Jiskoot, E. Mastrobattista, *J. Pharm. Sci.* **2020**, *3549*, 30785–30791.
- [9] D. J. Benton, A. G. Wrobel, P. Xu, C. Roustan, S. R. Martin, P. B. Rosenthal, et al., *Nature* **2020**, *588*, 327–330.
- [10] M. M. Lamers, J. Beumer, J. van der Vaart, K. Knoops, J. Puschhof, T. I. Breugem, et al., *Science* **2020**, *369*, 50–54.
- [11] F. Qi, S. Qian, S. Zhang, Z. Zhang, *Biochem. Biophys. Res. Commun.* **2020**, *526*, 135–140.
- [12] A. Iwasaki, R. Medzhitov, *Science* **2010**, *327*, 291–295.
- [13] R. L. Coffman, A. Sher, R. A. Seder, *Immunity* **2010**, *33*, 492–503.
- [14] U. Wille-Reece, C. Wu, B. J. Flynn, R. M. Kedl, R. A. Seder, *J. Immunol.* **2005**, *174*, 7676–7683.
- [15] U. Wille-Reece, B. J. Flynn, K. Loré, R. A. Koup, R. M. Kedl, J. J. Mattapallil, et al., *Proc. Natl. Acad. Sci. USA* **2005**, *102*, 15190–15194.
- [16] H. Hemmi, T. Kaisho, O. Takeuchi, S. Sato, H. Sanjo, K. Hoshino, et al., *Nat. Immunol.* **2002**, *3*, 196–200.
- [17] L. Nuhn, N. Vanparijs, A. De Beuckelaer, L. Lybaert, G. Verstraete, K. Deswarte, et al., *Proc. Natl. Acad. Sci. USA* **2016**, *113*, 8098–8103.
- [18] J. De Vrieze, B. Louage, K. Deswarte, Z. Zhong, R. D. Coen, S. V. Herck, et al., *Angew. Chem. Int. Ed.* **2019**, *58*, 15390–15395; *Angew. Chem.* **2019**, *131*, 15535–15541.
- [19] S. Van Herck, K. Deswarte, L. Nuhn, Z. Zhong, J. P. Portela Catani, Y. Li, et al., *J. Am. Chem. Soc.* **2018**, *140*, 14300–14307.
- [20] S. P. Kasturi, I. Skountzou, R. A. Albrecht, D. Koutsonanos, T. Hua, H. I. Nakaya, et al., *Nature* **2011**, *470*, 543–547.
- [21] G. M. Lynnn, R. Laga, P. A. Darrah, A. S. Ishizuka, A. J. Balaci, A. E. Dulcey, et al., *Nat. Biotechnol.* **2015**, *33*, 1201–1210.
- [22] Y. Chen, S. De Koker, B. G. De Geest, *Acc. Chem. Res.* **2020**, *53*, 2055–2067.
- [23] H. Liu, K. D. Moynihan, Y. Zheng, G. L. Szeto, A. V. Li, B. Huang, et al., *Nature* **2014**, *507*, 519–522.
- [24] R. Rathnasinghe, S. Strohmeyer, F. Amanat, V. L. Gillespie, F. Krammer, A. García-Sastre, et al., *Emerg. Microbes Infect.* **2020**, *9*, 2433–2445.
- [25] N. M. Shukla, S. S. Malladi, C. A. Mutz, R. Balakrishna, S. A. David, *J. Med. Chem.* **2010**, *53*, 4450–4465.
- [26] S. Lienenklaus, M. Cornitescu, N. Ziętara, M. Łyszkiwicz, N. Gekara, J. Jabłońska, et al., *J. Immunol.* **2009**, *183*, 3229–3236.
- [27] A. Wajnberg, F. Amanat, A. Firpo, D. R. Altman, M. J. Bailey, *Science* **2020**, *370*, 1227–1230.

Manuscript received: November 17, 2020

Revised manuscript received: December 24, 2020

Accepted manuscript online: January 19, 2021

Version of record online: March 11, 2021